# Optimization potential of the wire sawing process for multicrystalline silicon

**Thomas Kaden**, **Elena Ershova**, **Marcel Fuchs**, Fraunhofer THM, Freiberg, Germany & **Rajko B. Buchwald**, Meyer Burger (Switzerland) AG, Thun, Switzerland

ABSTRACT
As the diamond wire sawing process becomes increasingly important also for the wafering of multicrystalline silicon, a basic understanding of the material properties that influence the sawing performance becomes necessary. The position of the bricks in the multicrystalline ingot and the role of inclusions in the micrometer range as well as the orientation of the bricks in the wire web were investigated in detail. It is shown that an adaption of the brick sorting prior to wafering can be used to optimize the diamond wire sawing process in terms of increased throughput or lower wire consumption.

## Introduction

Today, silicon solar cells are still produced in almost equal shares from mono- and multicrystalline silicon wafers. For monocrystalline silicon the Czochralski-growth (Cz-Si) is the standard technique. In the case of multicrystalline silicon the so-called high performance multicrystalline silicon (HPM-Si) has become the standard base material. While diamond wire sawing (DWS) of monocrystalline silicon is currently being established as the industrial standard with a perspective of core wire diameters even below 70µm, DWS of multicrystalline silicon (mc-Si) is proving to be more challenging. This is due to the material properties of mc-Si, which are determined by a higher concentration of impurities and the presence of inclusions in comparison to Cz-Si. Furthermore, the standard acidic texturing of mc-Si wafers produced by DWS turns out not to be appropriate, since the onset of the etching process is too slow on the shinier DWS wafer surface.

## High performance multicrystalline silicon (HPM-Si)

The material quality of multicrystalline silicon was significantly improved by developing a directional solidification process with seeded growth, which drastically reduces the density of dislocations [1]. This so-called high performance multicrystalline silicon (HPM-Si) is now the standard multicrystalline base material for the solar cell production. Using n-type base doping, conversion efficiencies up to 21.9% have been demonstrated recently [2]. Although HPM-Si shows a high electrical quality, there are still impurities present in the material similar to standard mc-Si, which influence the wire sawing process.

## Wire sawing technologies

In general, two techniques for multi-wire sawing of crystalline materials exist. In loose abrasive sawing (LAS) a brass-coated steel wire is used in combination with a cutting fluid (the so-called slurry) consisting of a carrier fluid (typically PEG-200) and SiC as loose abrasive particles with a defined grain size (F600 or F800). The wire can be straight or structured, whereby the structured wire allows for higher feed rates. The main abrasion process is the brittle fracture of silicon due to a three-body interaction process with the SiC particles and the wire [3-5].

The second technique is the fixed abrasive diamond wire sawing (DWS), where the crystalline material is cut by diamond particles that are embedded in a nickel or resin coating on a steel core wire. A scheme of the DWS

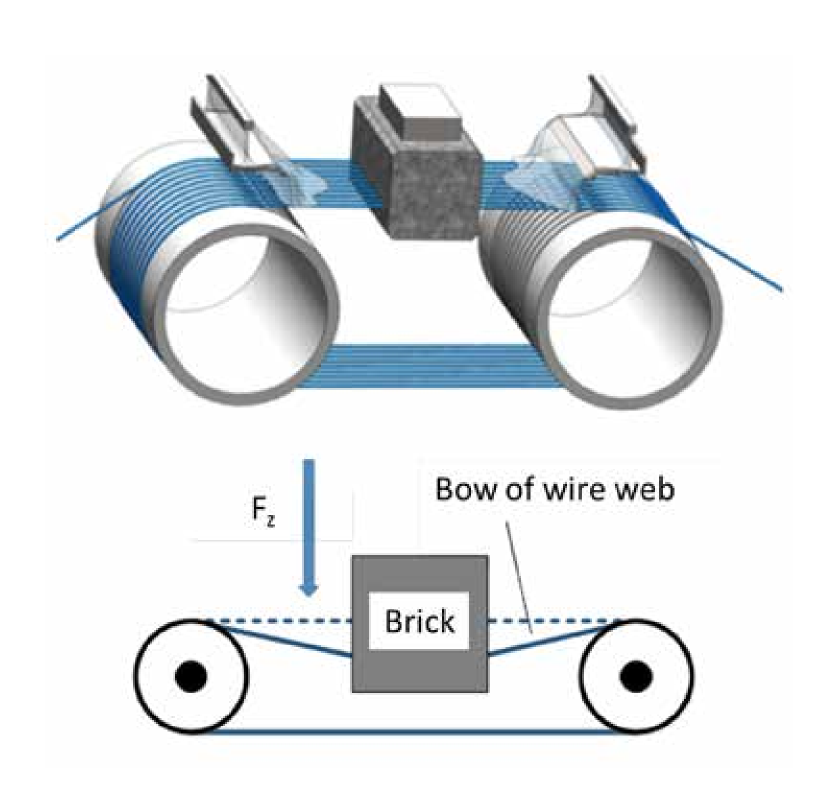


Figure 1. Scheme of diamond wire sawing and bow of wire web.

Materials

principle is depicted in Fig. 1. The wire web is moved in oscillation mode (forward/backward); in each forward step a certain amount of new diamond wire is added to compensate for the wire wear. The nozzles above the wire web are used to deliver the water-based cooling medium. The brick is moved through the wire web with defined feed rate in z-direction. Since feed rate and material removal rate are not equal, a bow of the wire web develops during the process which is represented by the force in feed direction $F_z$ (see Fig. 1).

The material removal in this technique is dominated by the ductile abrasion process, which yields shinier wafer surfaces compared to wafers prepared by the FAS technique [6, 7]. DWS allows for highly efficient processes, because higher feed rates are possible, cheap water-based coolants are used as cooling liquid and the kerf loss can be further reduced by the use of thinner wires. Today, 70µm core wire diameters are used in industrial production. An SEM image of such a wire is shown in Fig. 2. Furthermore, DWS offers the potential of kerf recycling, which is currently a widespread topic of research.

Our previous findings in slurry sawing processes revealed differences in the cutting efficiency of bricks from different positions in a multicrystalline silicon ingot. Surprisingly, cutting of bricks from the centre of the ingot turned out to be less efficient than cutting of bricks from the ingot edges and corners, respectively. This is demonstrated by the higher normal force $F_z$ developing during the sawing process as shown in Fig. 3 for sawing processes of each two bricks from the relevant positions of a mc-Si ingot. Typically, there are more impurities present in the edges and corners of the ingot due to diffusion from the crucible. However, the concentration of specific impurities that are less present in the edge and corner bricks might be the main influence on the sawing performance. In the following, bricks from different ingot positions were investigated in DWS processes in order to find out the optimization potential for the industrial wafer production and to determine the main influences on the wire sawing performance.

## Diamond wire sawing of HPM-Si from dedicated ingot positions

HPM-Si ingots from one dedicated manufacturer were considered for the investigations. Bricks from different positions in a G5 mc-Si ingot, i.e. from

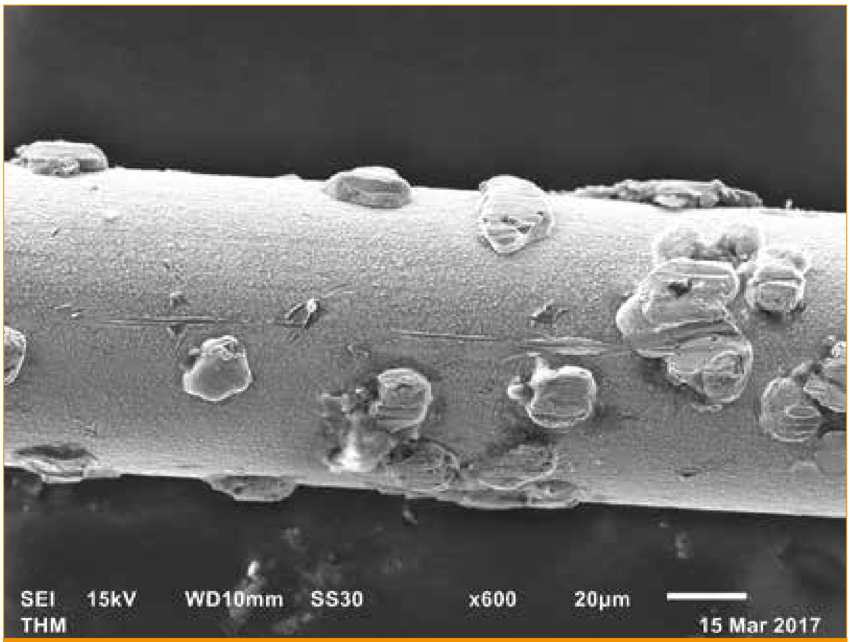


**Figure 2. SEM image of a diamond wire with 70µm core diameter and a grit size of 8-12µm.**

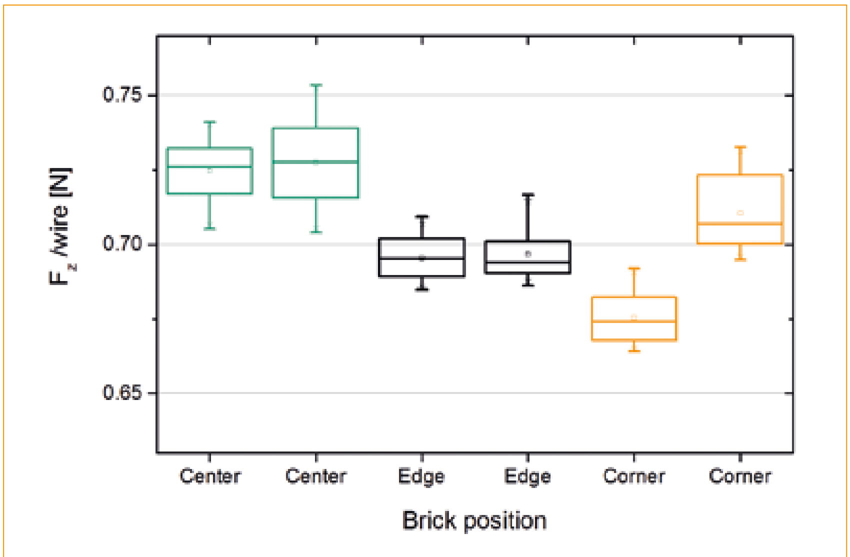


**Figure 3. Normal force $F_z$ during slurry sawing processes of multicrystalline bricks from different ingot positions.**

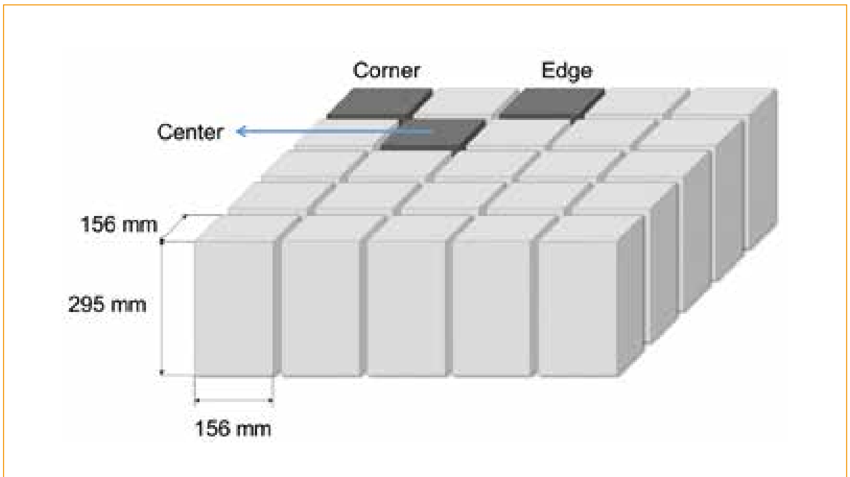


**Figure 4. Scheme of the investigated bricks from different positions in a G5 mc-Si ingot.**

the corner, edge and centre (see Fig. 4) were investigated in lab scale sawing experiments on a Meyer Burger DS 264 wire saw in diamond wire set-up. A monocrystalline Cz-Si ingot was used as reference. The experiments were done with a silicon load length of 295mm, a 120µm core wire and a diamond grit of 8-16µm at a wire speed of 18 m/s, a wire tension of 28N and a feed rate of 0.55mm/min. Throughout the whole cutting process the forces in three dimensions were monitored using a 3D piezo dynamometer. The normal force $F_z$, i.e. the force in feed direction, was used to assess the sawing processes for the different bricks. The magnitude of $F_z$ is a measure of the bowing of the wire web under the brick and thus reflects the cutting efficiency.

## Pre-characterization of the bricks

Prior to the wafering processes, the bricks were inspected by IR transmission with the standard resolution of 200µm. As it can be seen in Fig. 5, no inclusions are visible at this resolution; these bricks would thus pass the inspection control in the industrial wafering chain. The resistivity of all HPM bricks was in the range of 3-10Ωcm. The ingot position of the bricks was unambiguously determined by carrier lifetime mappings of slabs from the bottom and top of the bricks and can be seen by the extension of the so-called red-zone of low carrier lifetime (see Fig. 6).

## Characterization of wafering process and resulting wafer quality

Bricks of the same silicon load length of 295mm were cut with equal process parameters. Thus, the normal force $F_z$ is a measure for the cutting efficiency of the material. As it can be seen in Fig. 7, $F_z$ is the highest in case of the centre brick, for the corner and edge brick a significantly lower force develops in the course of the sawing process. The maximum $F_z$ is about higher 55% for the centre brick compared to the corner brick. For all HPM-Si bricks $F_z$ is higher in comparison to the reference Cz-ingot. These results confirm our findings on ingots of the same manufacturer using slurry sawing processes. However, the differences between the centre brick and bricks from the ingot edge or corner are even more pronounced in DWS. This is likely due to the higher feed rate used in the DWS process and probably also because of the different wear mechanism of the diamonds compared to the SiC particles in the slurry.

The resulting wafer thickness for each brick is depicted in Fig. 8. The thickness correlates with $F_z$, the higher the force the lower is the wafer thickness. With a higher wire wear (at higher $F_z$) the effective wire diameter, which is the core diameter plus the double mean grit size, becomes smaller. Thus the created sawing channel is also smaller, resulting in thicker wafers. Consequently, the reference Cz-ingot yields the thinnest wafers.

An important measure for the quality of the wafers is the total thickness variation (TTV). A higher force in the sawing process results in an increased TTV (see Fig. 9). The correlation is given for the HPM-Si bricks, the reference Cz-brick shows a slightly increased TTV. We explain this by minor wire distortion effects during the cutting-in of the pseudo-square Cz-bricks, for which the sawing process was not optimized. Furthermore, the mechanical stability of the wafers was tested by the four-line bending test. No differences within the measurement accuracy where found between the different HPM-Si bricks, neither in the as-sawn state nor in the damage-


Figure 5. IR transmission images of the mc-Si bricks with standard resolution of 200µm.

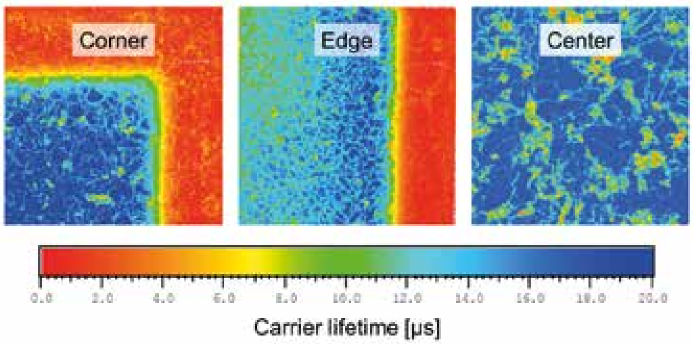


Figure 6. Carrier lifetime mappings of the bottom slabs prove the ingot position of the bricks.

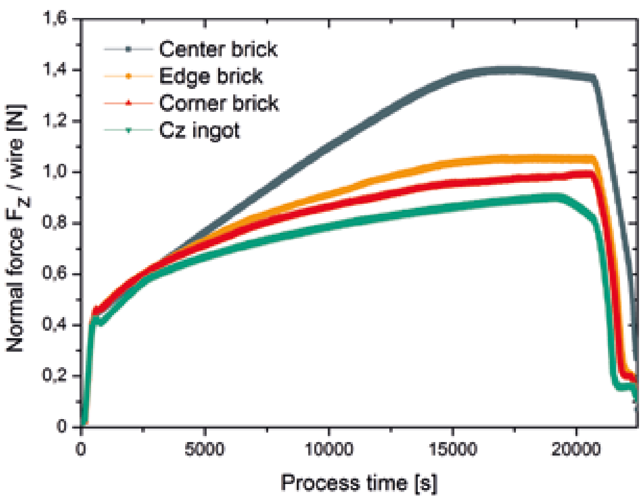


Figure 7. Normal force $F_z$ over the whole process time.

etched state. However, the reference Cz-wafers turned out to be more stable as it is expected.

## Influence of different material properties

After finding these significant differences in the cutting efficiency of HPM-Si bricks from different ingot positions, which material property has the dominant effect on the sawing process should be clarified. No correlation was found between $F_z$ and the concentration of interstitial oxygen and substitutional carbon as determined by FTIR spectroscopy. The average grain size as well as the number of relevant grain boundaries was determined as a function of the brick height by X-ray diffraction ("Laue scanner"). The differences of these crystal structure properties between the investigated bricks do not reveal a correlation to $F_z$, too.

We attribute the differences in the cutting efficiency to the presence of silicon nitride ($Si_3N_4$) and silicon carbide (SiC) precipitates, which were found by IR microcopy in the bottom and top slabs of the bricks. An example of $Si_3N_4$ needles in the corner brick are shown in Fig. 10. The majority of precipitates found have been $Si_3N_4$ needles that are likely originating from the crystallization crucible. SiC precipitates were only rarely found.

By automated determination of the precipitate area and counting the number of inclusions in the bottom and top slabs of the different HPM-Si bricks, the median precipitate area was calculated, yielding significant differences. The mean precipitate area in the centre brick is almost twice the median area in the edge and corner bricks. This correlates with the maximum normal force $F_z$ occurring in the wire sawing process (see Fig 11).

## Industrial scale wire sawing of HPM-Si with 70µm core diameter

A larger amount of HPM-Si bricks of the same manufacturer as in the experiments presented above was investigated using a state of the art Meyer Burger DS288 diamond wire saw. The full load length of the machine was used by mounting two ingots in series. The experiments were done with a 70µm core wire, a diamond grit size of 6-12µm and an overall process time of 150 minutes with a wire speed of 30m/s and a wire consumption of about 1.8-2.0m/wafer.

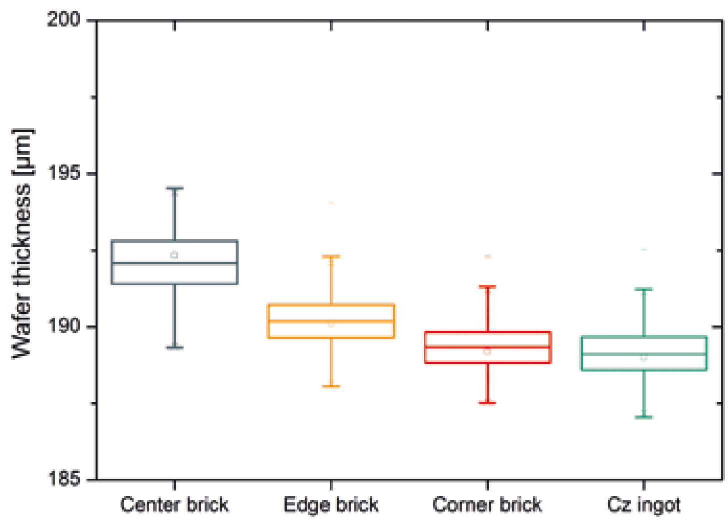


**Figure 8. Thickness of the resulting wafers, each box comprises about 830 wafers.**

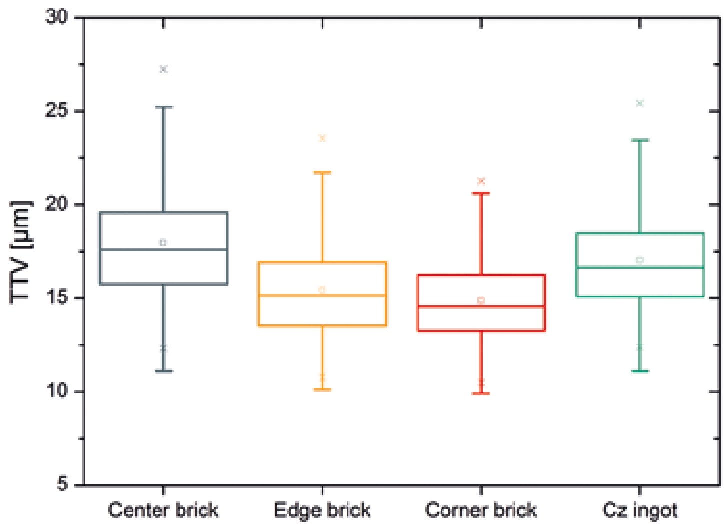


**Figure 9. Total thickness variation (TTV) of the resulting wafers, each box comprises about 830 wafers.**

| Configuration FB to MB | Maximum cut area [cm²/m] | Mean TTV [µm] | Saw mark depth [µm] |
|---|---|---|---|
| Bottom → Top / Top → Bottom | 156 | 6.4 | 12.6 |
| Top → Bottom / Bottom → Top | 185 | 9.5 | 15.8 |
| Top → Bottom / Bottom → Top | 185 | 11.2 | 19.0 |
| Bottom → Top / Bottom → Top | 185 | 6.9 | 13.9 |

**Table 1: Configuration of the HPM-Si bricks in full load cuts and resulting wafer TTV and saw mark values.**

## Pre-characterization of the bricks

The bricks were investigated with a high resolution IR transmission system with a spatial resolution of 18µm. Exemplarily shown are point- and needle-like inclusions in a HPM-Si brick in Fig. 12. Different bands of these inclusions are displayed by red to blue color in the images.

After unambiguously determining the bottom and top of the bricks, different configurations of brick arrangements were tested in full load cuts in industrial DWS processes. All bricks contained a section of inclusions near the top of the brick and a second band near the bottom of the brick. The configurations of the bricks from the fixed bearing of the machine (FB) to the movable bearing (MB) are shown Table 1. The FB side is the new wire entry side of the wire web.

In the first configuration a maximum cut area of 156cm²/m wire length was used yielding a mean TTV of 6.4µm. For the following three configurations, a higher maximum cut area of 185cm²/m wire length was used in order to yield a more pronounced effect of the inclusions on the wafer quality. It turns out that configuration starting with the bottom of the first brick from the FB side and arranging the bottom of the second brick also towards the FB side is the most favourable regarding the mean TTV of the wafers. The number of saw marks correlates with the TTV values.

For the second configuration, the influence of the precipitate bands within the bricks on the wafer quality is shown in detail in Fig. 13. The first precipitate band (top of brick #1) looking from the new wire entry side does not have an effect on TTV or saw marks. The precipitate band in the bottom regions of brick #1 and #2 drastically influence the wafer quality as it can be seen by higher thickness values (red color) and more pronounced saw marks. The precipitate band in the top region of brick #2 (MB side) does again not influence the wafer quality, as shown by standard wafer thicknesses (green color) and unremarkable saw mark depths. Generally, the bottom regions of the ingot appear to be harder and have the highest impact on the wafer quality in this configuration.

## Conclusion

The inspection and characterization of multicrystalline silicon bricks plays an important role for the optimization of the diamond wire sawing process. It turned out that the standard IR transmission with 200µm spatial resolution is not sufficient to detect all impurities, which have a relevant influence on the cutting efficiency of the material.

Comparing bricks from different ingot positions in laboratory-scale DWS experiments, the cutting efficiency shows significant differences as demonstrated by monitoring the force in feed direction over the entire process time. For a specific crystal manufacturer within this work, the bricks from the edges and corners of an HPM-Si ingot can be more easily cut compared to bricks from the ingot centre. This was mainly attributed to the presence of silicon nitride precipitates of different size within these ingots as characterized by IR transmission microscopy. In the case of other crystal producers the situation might be different. If the precipitates in the edge regions of the ingot would be larger, depending on the melt convection during the crystallization process, the cutting efficiency of edge and corner bricks will be lower compared to centre bricks.

The findings offer the potential for process optimization with a cost reduction potential. Thus, a presorting of bricks prior to the wafering could be established, which distinguishes centre and edge/corner bricks, given that the precipitate distribution is known. After presorting, adapted processes regarding feed rate or wire consumption can be applied for the two groups of bricks.

The relevant precipitate distribution can be monitored with a high resolution IR transmission measurement of the bricks, offering a spatial resolution of 18µm. Such a system was used to identify bands of point- and needle-like precipitates within HPM-Si bricks. The position of the precipitate band correlates with the appearance of higher wafer TTV values and saw marks on the wafer surface.

The configuration of bricks regarding the position of brick bottom and top also plays a role when using the full load length on state-of-the-art diamond wire saws with 70µm wire core diameter in industrial processes. A serial arrangement in the order brick bottom to top looking from the fixed bearing to the movable bearing of the machine turned out to be favourable for the crystals of the manufacturer that were investigated here. In general, a further reduction of the size of precipitates, especially of silicon nitride needles and SiC clusters, is desired in order to further improve the cutting efficiency of multicrystalline silicon bricks in diamond wire sawing.

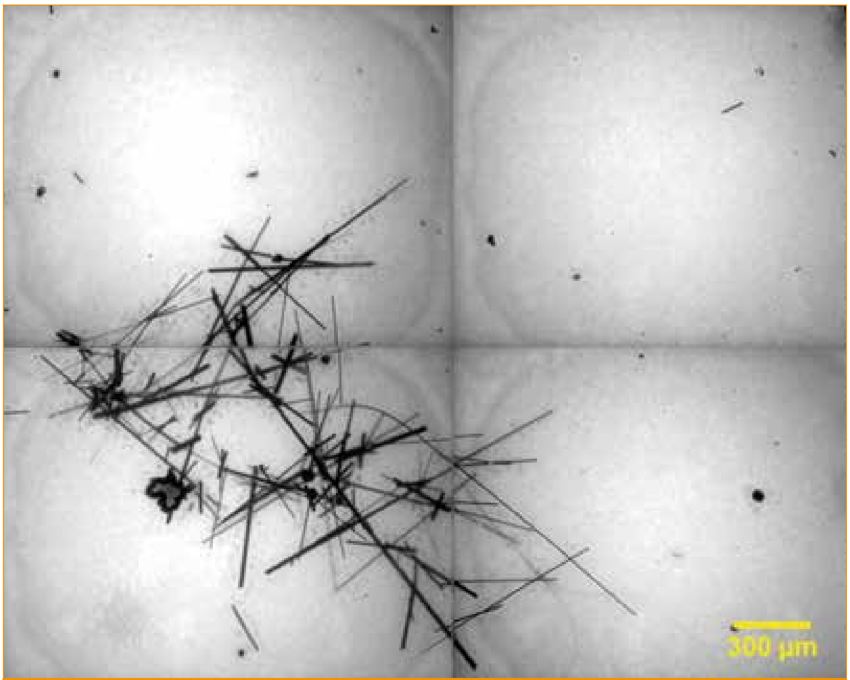


**Figure 10: IR transmission microscopy of the corner brick bottom slab showing an aggregation of $Si_3N_4$ needles.**

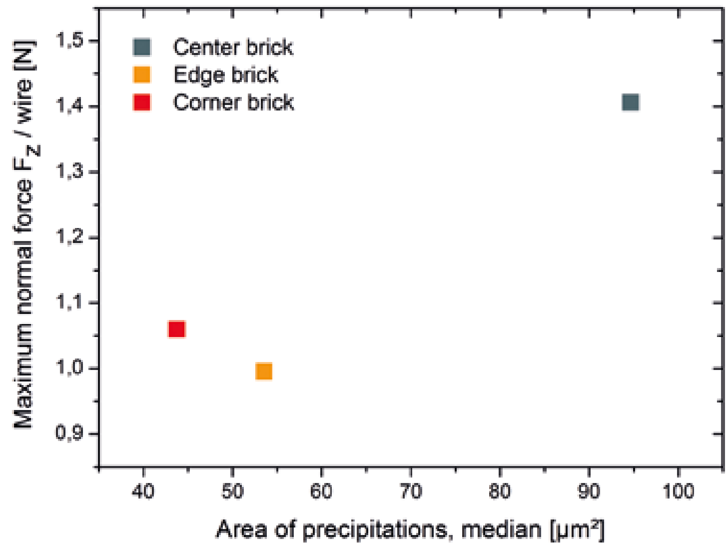


**Figure 11. Correlation of $F_z$ and the median precipitate area in the bottom and top slabs from the different HPM-Si bricks.**


## Acknowledgement

Parts of the research were funded by the Federal Ministry for Economic Affairs and Energy with in the project "DIANA" (Contract No. 0324087B), which is gratefully acknowledged.


## References


[1] Riepe, S. 2015, "Development of multicrystalline silicon for 20% efficient n-type solar cells", Proc. of 31st EU-PVSEC, pp. 295-299.

[2] Beneck, J. 2017, "High-Efficiency n-Type HP mc Silicon Solar Cells", IEEE Journal of Photovoltaics, Vol. 7, No. 5, pp. 1171-1175.

[3] Möller, H.J. 2004, "Basic Mechanism

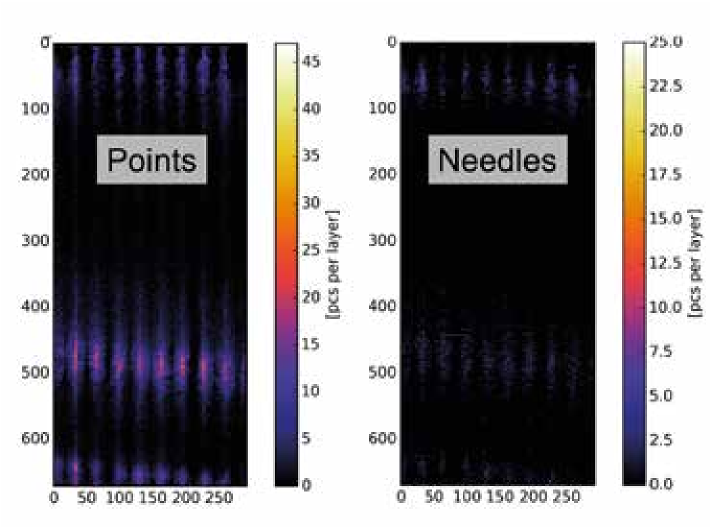


**Figure 12. Bands of point- and needle-like defects detected by high-resolution IR transmission.**

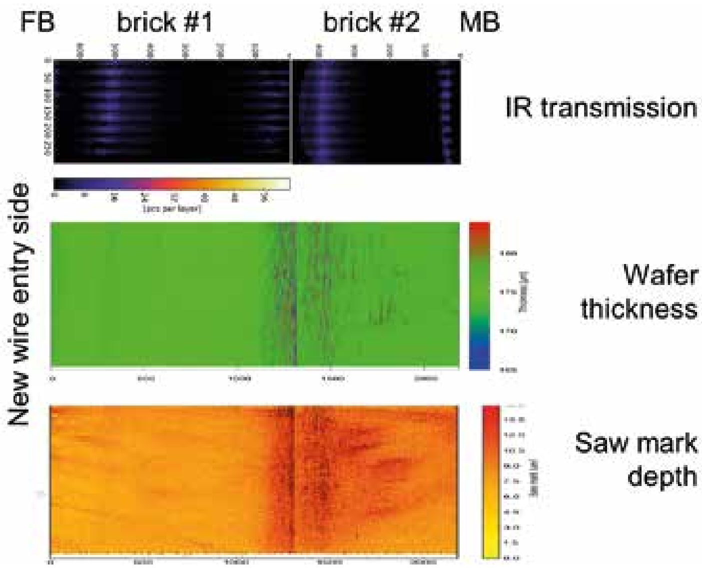


**Figure 13. Correlation of precipitate bands with wafer thickness and saw mark depth in the second configuration.**


and Models of Multi-Wire Sawing", Advanced Engineering Materials, Vol. 6, No. 7, pp. 501-513.

[4] Behm, T. 2011, "Challenges of the wire saw wafering process", Photovoltaics International, No. 11, pp. 36-47.

[5] Schumann, M. 2009, "The solar cell wafering process", Photovoltaics International, No. 5, pp. 53-59.

[6] Buchwald, R. 2013, "Analysis of the sub-surface damage of mc- and Cz-Si wafers sawn with diamond-plated wire", Energy Procedia, Vol. 38, pp. 901-909.

[7] Würzner, S. 2017, "Characterization of the Diamond Wire Sawing Process for Monocrystalline Silicon by Raman Spectroscopy and SIREX Polarimetry", Energies, Vol. 10, 414.


## About the Authors

**Thomas Kaden** studied applied natural science at TU Bergakademie Freiberg and received his Ph.D. in physics in the photovoltaics group of Prof. H.J. Möller. After working on silicon material topics in the R&D department at Q-Cells S.E. in Bitterfeld, he joined Fraunhofer THM in 2012. Starting with solar module activities, he later joined the wafering group. Since 2016 he is Head of the Group THM Wafering.

**Elena Ershova** holds a diploma in information technology and systems from TU Wolodga (Russia) and performed the majority of experiments presented here during her bachelor thesis at Fraunhofer THM. In July 2017 she obtained a bachelor of science in environmental engineering from TU Bergakademie Freiberg.

**Marcel Fuchs** worked as an operator in wafer and solar cell production and was production supervisor of a wafering company before he joined Fraunhofer THM as senior technician in wafering in 2012. He operates the wire sawing machines and gives valuable input in developing and improving sawing processes for different kind of hard-brittle materials.

**Rajko B. Buchwald** studied applied natural science at the TU Bergakademie Freiberg. He received his Ph.D. in 2010. In 2010 he joined Fraunhofer THM in Freiberg. Under the lead of Prof. Möller he helped making the centre operational to investigate and improve diamond wire slicing processes on industrial scale. After two years as Head of Group Wafering he moved to Meyer Burger (Switzerland) AG in 2016.

## Enquiries


Dr. Thomas Kaden
Fraunhofer Technology Centre for Semiconductor Materials THM
Am St.-Niclas-Schacht 13

09599 Freiberg, Germany
Tel.: +49-3731-2033 166

Email: thomas.kaden@thm.fraunhofer.de
Web: www.thm.fraunhofer.de